Effects of solution concentration on properties of P3HT films

Daniel Keane

Research Option Thesis

School of Chemical & Biomolecular Engineering

Georgia Institute of Technology

Spring 2018

Research Advisors: Dr. Martha Grover & Dr. Elsa Reichmanis

Research Mentor: Michael McBride

I. ABSTRACT

Past experiments have studied Poly(3-hexylthiophene-2,5-diyl) (P3HT) by examining the roles of parameters including molecular weight, aggregation methods, and dispersion method on device performance. However, the role of the P3HT solution concentration on the polymer's properties are not fully understood. This research examined the role of polymer solution concentration on the properties of UV-treated P3HT. P3HT of two different molecular weights was examined, and three different concentrations each were examined for each weight. To characterize a given weight-concentration combination, electrical capabilities of the films were measured on FETs, UV-vis measurements were taken of solution and films, and films were examined under Atomic Force Microscopy (AFM). The results suggest that the long-range order of P3HT films is closely related to the solution concentration. For films created from higher solution concentrations, more fibers in films of P3HT are aligned in the same direction and a larger fraction of polymer in the solution is aggregated. Of the three solution concentrations tested, the middle concentrations performed the best electrically, suggesting that solubility factors, chain count, and viscosity strongly affect the resulting film's properties.

Table of Contents

II. ACKNOWLEDGEMENTS

Throughout my 3 semesters of work, Michael McBride has provided me with guidance and recommendations. I would have been lost without his help. I also want to extend a special thanks to Dr. Martha Grover for providing me with the opportunity to perform research under her supervision. Finally, I'd like to thank Dr. Elsa Reichmanis for providing me access to her lab and providing feedback when requested.

III. LITERATURE REVIEW

Semiconducting organic polymers are essential in the growing field of organic electronic devices. Though the electrical performance of organic semiconductors cannot compete with that of inorganic ones, significant developments made in the past decade have greatly improved the charge carrier mobility of organic semiconductors.[1] Solution-processable, cost effective, flexible, and lightweight, these conjugated polymers have the potential to lead to a new era of electronics including organic field-effect transistors (OFETs), organic photovoltaics (OPVs), and light emitting diodes (OLEDs).[2-4]

While a large majority of research focuses on OFETs, the results may be applicable to the field of organic electronics in general. An important part of all electronics is the field-effect transistor (FET), a device consisting of three electrodes called the source, drain, and gate. A semiconductor channel connects the source and drain, while the gate is separated from the channel by an insulating layer. An electric current enters the channel through the source and exits through the drain at the other end, but applying a voltage to the gate can produce an electric field that affects the current. Hence the name: field-effect transistor. Basically, by turning on and off the voltage on the gate, the flow of the charge carriers can be controlled.[5]

In 1987, Koezuka, Tsumara, and Ando published a paper documenting the first field-effect transistor created using polythiophene as the semiconducting material. The transistor in their study was composed of a gold electrode on a layer of silicon dioxide with a film of the polymer in between the electrodes; this design, often with slight modifications, serves as the basis for most transistors studied in the field.[6] With this design in mind, research in this field attempts to optimize the processing of the organic semiconducting polymers to maximize charge carrier mobility.

The charge mobility in semiconducting polymers is largely determined by the chemical structure, intermolecular packing, and long-range order.[7-8] Charge travels better along individual fibers than in between two, but long fibers do not necessarily show higher charge transport.[9] Charge can be transported across these chains and hop from one chain to another, but in the grain boundaries between chains, the charge carriers scatter, leading to reductions in the mobility.[10]

Numerous semiconducting polymers, both n- and p-type semiconductors, have been studied as potential candidates for organic electronics.[3] Perlylene diimides (PDIs) are a commonly studied class of p-type semiconductors that participate in charge transfer through hole transfer.[11] When PDIs are solution processed, portions of adjacent molecules' π-molecular orbitals overlap and assemble into columnar stacks.[11] These nanofibers are highly ordered and serve as the primary means of charge transport in the produced films.[10] Poly(3-hexylthiophene-2,5-diyl) (P3HT) is a frequently studied alternative to its PDI-derivative counterparts.[11] P3HT is readily available, has high solubility at low temperatures, and easily organizes into semi-crystalline structures, making it a model polymer to study.[12]

Continual progress has been made in recent years in optimizing the treatment process in order to achieve high charge-carrier mobility.[10] Most of the work with P3HT attempts to manipulate the long-range order to improve crystalline structure since higher directional alignment of P3HT has led to higher mobilities.[8] Details of the processing, including the solvent identity, aggregating treatment, and deposition method, have had strong impacts on the properties of the nanofibers.[8, 13] Unfortunately, the research in this field is often difficult to reproduce. The systems involved are complex and many variables affect the results, so the values of the charge-carrier mobility often vary over several orders of magnitude, even for the same experimental procedure.[14]

In the studies discussed here, the two dominant methods for solution deposition have been spin-coating and blade coating, but several other methods have been tried. A method of creating films, suggested by Liu *et al*., involved placing a glass slide over a drop of solution and applying pressure; well-ordered films were produced, but the study did not test electrical properties.[10] Of the two dominant deposition methods, spin-coating was the first proposed; the process involves dripping solution onto a spinning transistor, spreading it due to centrifugal force. Blade coating was later proposed for solution deposition; in blade coating, a razor is lowered to a surface, solution is pipetted ahead of the blade, and the blade is moved forward across the surface. This process uses shear force to draw the solution across the transistor, orienting the nanofibers in the direction of shear force and creating a well-ordered film.[13]

Chu *et al*. demonstrated the significant differences in the films produced through these two methods. Analyzing both atomic force microscopy (AFM) images and analysis of cross-polarized UV-vis spectra, Chu *et al*. showed that films prepared through blade coating were consistently more ordered than those prepared with spin-coating. Blade-coated transistors showed higher mobilities than spin-coated transistors, whether the direction of blade coating was parallel or perpendicular to the transistor pathway.[8]

Chang *et al*. also analyzed the differences between blade- and spin-coating, coming to the same conclusion that blade coating was the more effective method of solution deposition. This study also observed significant changes in the films produced when the speed of blade coating was altered. After testing rates of 0.5, 1, 2, and 4 mm/s shear rates, the most ordered and best electrically-performing films were those produced using a blade speed of 2 mm/s.

Over the past several years, methods for aggregating P3HT have included solution aging, UV irradiation, sonication, and mixing with poor solvents.[12-13, 15] The method of using poor solvent

addition to aggregate the polymer was discussed by Scharsich *et al*. This study demonstrated that aggregation occurs when poor solvent is added to a solution of polymer dissolved in good solvent. More poor solvent led to greater aggregation, and a lesser volume of poor solvent was required to aggregate higher molecular weights. All solutions plateaued at some maximum aggregation, the largest of which was only 55% aggregated. The molecular weights of P3HT used in this study ranged from 5 to 19 kDa and were therefore lower than those in the study reported here.[15]

The potential of using low-intensity UV irradiation as the aggregating agent of P3HT was demonstrated by Chang *et al*. in a 2014 paper. As the solution was exposed to UV light for longer periods of time, an increase in aggregation of the polymer and an increase in the directional alignment of the fibers in film were observed through UV-vis measurements and AFM images, respectively. The mobilities of the created transistors appeared to increase logarithmically and plateau after about 8 minutes of UV irradiation. Since the molecular weight of the polymer has a significant impact on its properties, it is important to note that the molecular weights of the polymers used in this study were 19.7 kDa and 43.7 kDa.[12]

The potential of aging as the sole aggregating treatment of P3HT is demonstrated by Kleinhenz *et al*.[2] UV-vis measurements used to analyze the solution showed a progressive increase in the fraction of aggregated P3HT molecules with more aging. Furthermore, the directional alignment, determined through analysis of Cryo-TEM images of films, tended to increase with age.

Past experiments have examined the effects of altering several other parameters, but little data has been collected on the electrical impact of the polymer solution concentration. Past published experiments have pointed to a relationship between concentration and morphological features of the film, but optimization of the concentration for application to electronics has not

been examined. The purpose of this research is to optimize the concentration of solution-treated P3HT for application to organic electronics by maximizing electrical performance and directional order of produced films.

IV. INTRODUCTION

P3HT has a high solubility at low temperatures and self-assembles in solution.[12] Electron mobility in P3HT is heavily influenced by its fibril microstructure, including the intermolecular packing and long-range order.[7-8] Charge travels best along individual fibers so films with high mobilities generally have long-range order in their crystal structures.[8, 10] Progress has been made in recent years in optimizing the treatment of P3HT to achieve high charge-carrier mobility.[10] Details of the processing, including the solvent, treatment, and deposition method, have been shown to have strong impacts on the fibril structure of a P3HT film.[8, 13] To achieve this structure, the polymer must be treated in solution to induce aggregation and then be deposited in an ordered film.[8] Some common treatments are solution aging, UV radiation, sonication, and mixing with poor solvents.

Since UV-irradiation and aging were demonstrated to be effective methods of aggregating P3HT, the combination of the two has been frequently used to aggregate P3HT in solution. The use of both treatments allows for more aggregation than is achieved solely with UV irradiation, but is quicker than using only solution aging. The effectiveness is demonstrated by Chu in his 2016 paper.[8] The combination of UV-irradiation and solution aging as the solution treatment has thus been determined to produce the most promising results, and likewise, blade coating is shown to be the best method of film deposition.[12] Therefore, this experimental plan uses a combination of UV-irradiation, solution aging, and blade coating.

Numerous studies have altered process parameters and observed the effects, but little work has studied the role of solution concentration on a polymer film's microstructure. According to kinetic theory, high reactant concentrations lead to more collisions between molecules and therefore a faster reaction. However, steric hindrance between polymer chains can occur in highly concentrated solutions, resulting in the slowing of chain growth. The purpose of this research was to investigate how P3HT solution concentration affects the formation of films for application to organic electronics. Properties of P3HT fibers and films were analyzed at different concentrations, and trends were identified.

V. MATERIALS & METHODS

i. Preliminary Studies

Preliminary studies were conducted to gauge the effectiveness of different ranges of P3HT concentrations. Molecular weights of both 37 kDa and 95 kDa were examined. Each individual experiment investigated a slightly different range of concentrations but used the same analysis techniques. When presented, results from these short studies will include a description of the specific test conditions and how they influenced the experimental design moving forward.

ii. Experiment Details

Regioregular P3HT of two molecular weights—37 kDa and 95 kDa—was investigated. For the 37 kDa P3HT, concentrations of 2, 5, and 8 mg/ml were examined and for the 95 kDa polymer, concentrations of 2, 4, and 5 mg/ml were examined. These concentrations were specifically chosen to effectively explore the concentration's role. For the 95 kDa P3HT, the solubility limit is around 5 mg/ml of solvent, setting an upper bound to viable concentrations. Preliminary experiments suggested that solutions of 4 mg/ml produce effective films, so this

concentration was also tested. Third, a 2 mg/ml solution was created to compare to the 37 kDa solution of the same concentration.

The solubility limit of 37 kDa P3HT is much greater than that of the 95 kDa. Preliminary tests suggested that concentrations greater than 10 mg/ml were not effective. Thus, the highest concentration tested was 8 mg/ml. Furthermore, a concentration of 5 mg/ml was tested because it is commonly used for solutions of P3HT. Finally, a 2 mg/ml solution was tested; this solution's molar concentration is approximately equal to that of the 5 mg/ml 95 kDa P3HT solution.

iii. Solution Creation

For each concentration of P3HT tested, the proper amount of polymer was weighed and placed into a 50 mL vial, and 1 mL of chloroform was added. These solutions were then heated on a hotplate at 55°C for 30 minutes, or until all solid was dissolved, resulting in an orange solution. The solution was then removed from the hotplate and allowed to cool to room temperature. Next,

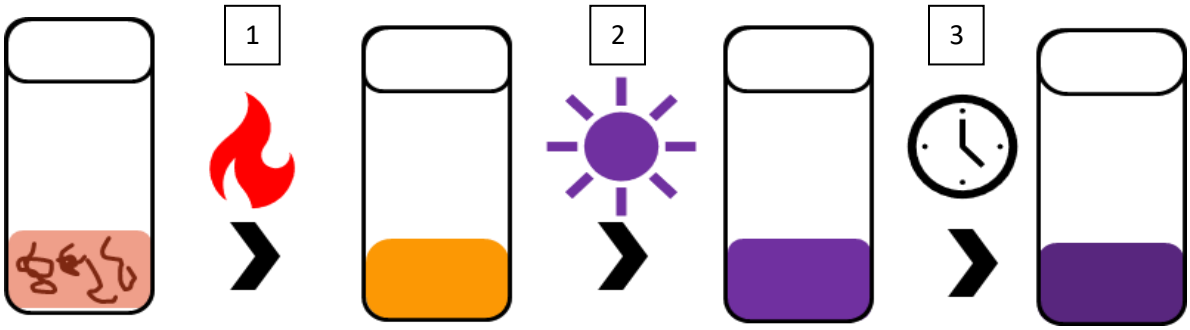

Figure 1. The treatment of the P3HT solutions. The polymer was dissolved in heated chloroform, treated with UV-irradiation, and then aged. Transition 1: P3HT is dissolved in $CHCl_3$ over heat. Transition 2: After cooling, the solution is treated with UV-irradiation for 8 minutes. Transition 3: The solution ages.

the solution was treated with Ultraviolet irradiation. A short-wave UV light source (Entela UVGL-15, 5 mW cm^{-2}, 254 nm) was placed on top of a room-temperature hotplate and a stir bar (Corning Inc) was placed in the vial. The vial was placed on top of the UV source, the stir rate was set to 300 rpm, and the UV light was turned on. The vial was stirred continuously on top of the UV light for 8 minutes, during which the solution turned to a dark purple. The UV source was found to heat

up during treatment, so after each trial, the light was turned off until cooled to room temperature in order to avoid affecting the samples.

iv. Blade coating

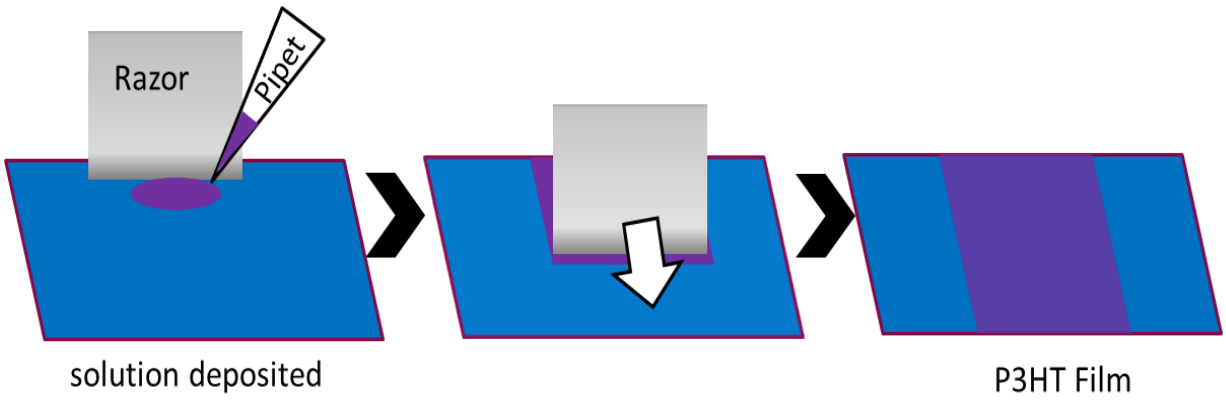

Figure 2. The method of blade coating. Solution is deposited in front of a razor blade and then drawn across the surface.

Blade coating was used to create films of this treated P3HT. A transistor was placed on a moving platform (A-LSQ150AE01, Zaber) and attached by vacuum. A razor blade was attached to the platform parallel to the transistor and lowered to a height of 5 µm. The platform was initially positioned to the left of the transistor and set to a speed of 2 mm/s. Solution (5 µL) was pipetted to the right of the blade and the platform was started. When the blade passed the right edge of the transistor, the platform and vacuum were switched off, and the transistor removed. This process is also performed to coat glass slides for UV-vis analysis.

v. Electrical Testing

To test the charge carrier mobility of a polymer film, an organic field-effect transistor with bottom-gate bottom-contact design was bladecoated using the previously described method. Chloroform was used to *pattern* the transistors, removing any polymer solution outside the intended coating. The transistor was then

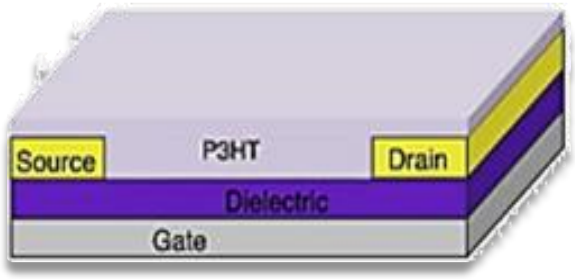

Figure 3. A diagram of an OFET with bottom-gate bottom-contact design.

placed in a vacuum oven at 50˚C for 12 hours to evaporate the chloroform. Lastly, the transistor was transferred to a nitrogen glovebox where its electrical capabilities were tested using an Agilent 4155c semiconductor parameter analyzer. The electrical testing specifications and analysis methods are described in Appendix A-III.

vi. Aggregate Fraction

UV-vis spectroscopy was used to measure the extent of aggregation in the P3HT solutions. First, a base spectrum was taken on an UV spectrometer (Agilent HP 8510 UV−vis spectrophotometer) with 30 µL of chloroform between two glass slides. To measure the polymer solution, samples of the solution were pipetted between glass slides and absorption spectra were gathered. Using the equation described in Appendix A-II, the aggregate fraction, or the percent of total chains in the solution that have grown into larger superstructures, was calculated.

vii. Dichroic Ratio

UV-vis spectroscopy was also used to take spectra of polymer films using a polarimeter. Pre-cleaned glass slides were blade-coated with P3HT solution, and a base spectrum was measured with a glass slide blade-coated with chloroform. For each P3HT-coated slide, UV measurements were taken with a cross-polarizer—one measurement at with the polarizer set to 0° and one at 90°. The ratio of the largest peaks in the two polarized measurements, called the dichroic ratio, measures the film's optical activity and has been previously correlated with the directional order of the polymer fibers.

viii. Atomic Force Microscopy (AFM)

To more effectively examine the microstructures of the polymer, AFM images were collected and analyzed. A Bruker Dimension Icon AFM system, in tapping mode with n-type silicon tips (HQ:NSC14, MikroMasch), produced clear images of the fibril structures in the films. The blade-coated transistors were observed under the microscope, providing further insight into the relationship between fibril order and electrical performance. An algorithm is used to identify the orientation of and gather statistics on the fibers. It is an effective tool in analyzing the microstructure, providing information on the direction and length of fibers.[16]

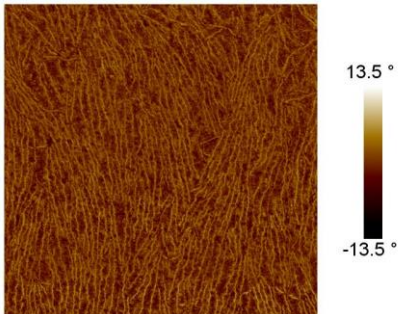

Figure 4. An example AFM image taken of a 5-um square of P3HT

VI. RESULTS & DISCUSSION

i. Preliminary Studies

Several short studies and stand-alone experiments were conducted to gain an initial understanding of the effect of concentration on the polymer solution and film. For both the 37 kDa and 95 kDa P3HT, solubility limits in $CHCl_3$ were investigated to determine plausible testing ranges for both molecular weights. It was determined that for the 95 kDa polymer, 5 mg/ml was near the upper limit of solubility and any further addition of polymer resulted in precipitation after UV-treatment and aging. Thus, this was determined to be the maximum viable concentration for this weight. For the 37 kDa P3HT, the solubility limits were much greater; 20 mg/ml solutions were successfully created and treated, but due to material costs, higher concentrations were unreasonable.

The first preliminary study observed the charge-carrier mobility for solutions of 95 kDa at five different concentrations: 1mg/ml through 5 mg/ml. The mobilities were tested after 3 days aging and are presented in Figure 5. There is a clear curve to the data that shows a peak charge-carrier mobility around a concentration of 4 mg/ml. This data was used to choose the concentrations of 95 kDa P3HT that would be further studied.

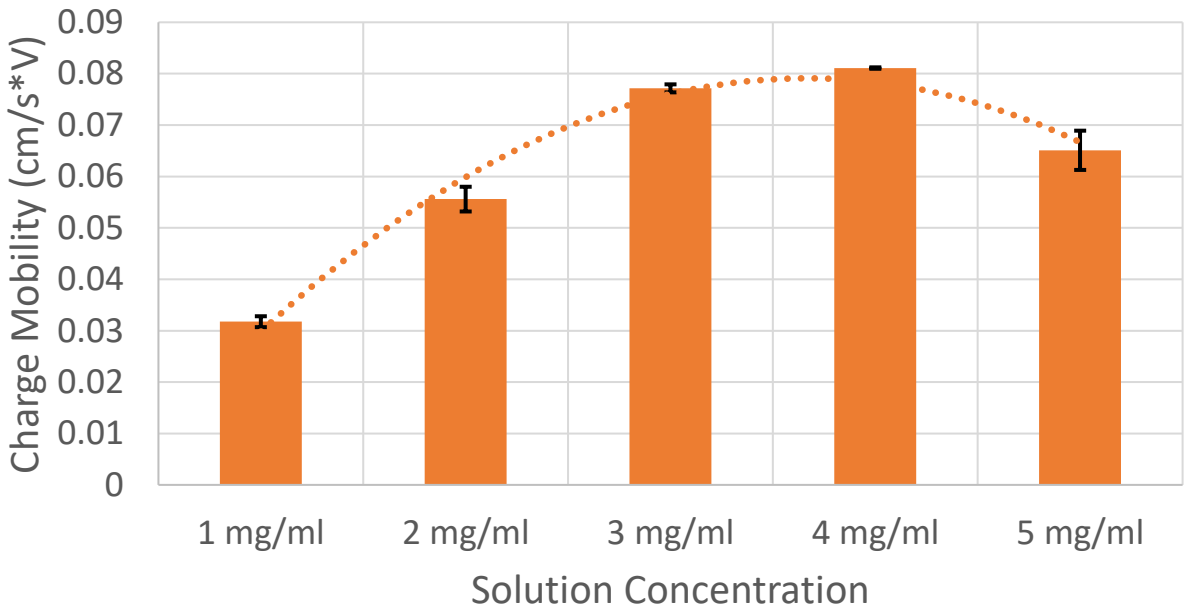

Figure 5. Mobility data for solutions of 95 kDa P3HT from a preliminary experiment. The data shows a clear trend in which the electrical capabilities peak around 4 mg/ml. Error bars show standard deviations over 4 data points for each trial.

Electrical properties of 37 kDa P3HT were also observed. Both the 10 and 20 mg/ml solutions failed to produce effective films, and were therefore deemed too concentrated for the study. These preliminary experiments provided some initial insight into viable concentration ranges and helped make decisions regarding the main study.

ii. Results: Aggregate Fraction, Dichroic Ratio, & Mobility

The solution, film, and electrical properties of treated P3HT at three different solution concentrations for both molecular weights of 37 kDa and 95 kDa. Several methods were used to characterize the polymer both in solution and in thin films.

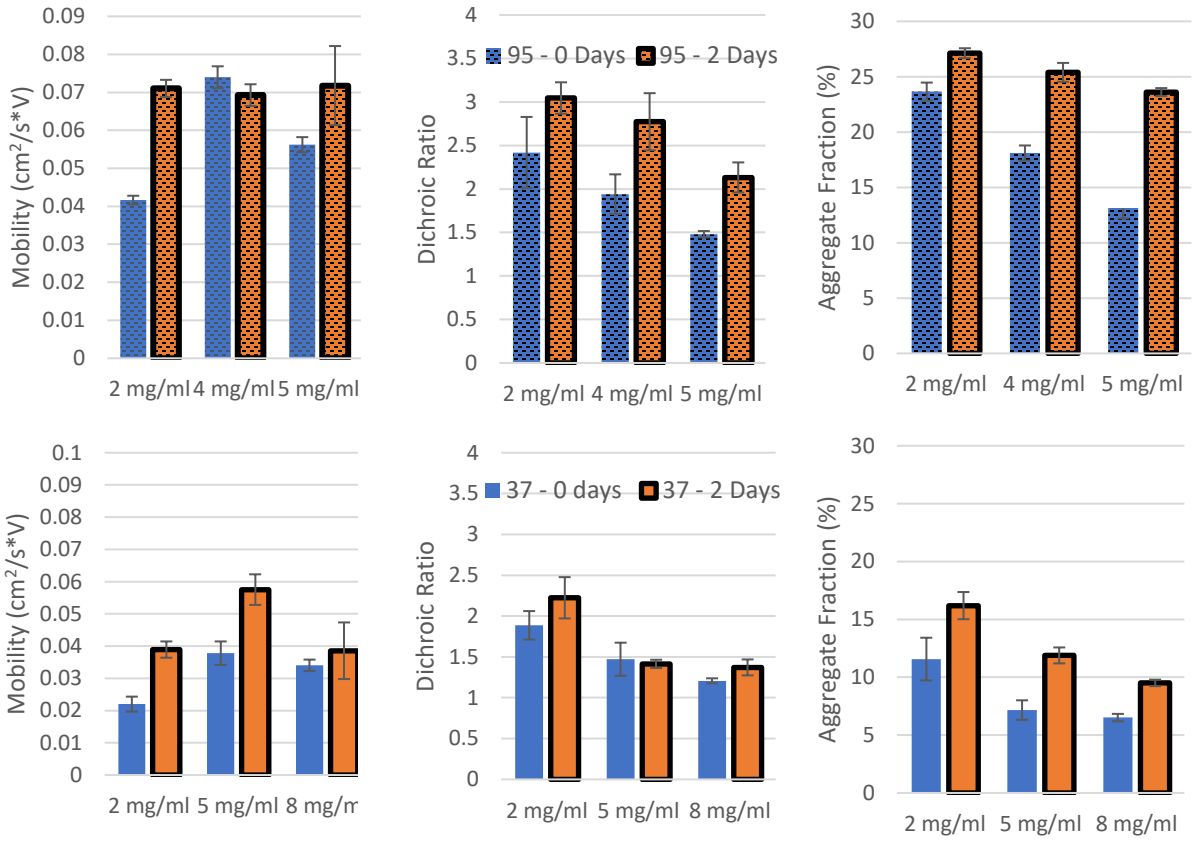

Figure 6. *Top Left*: 95 kDa Mobilities. *Top Middle*: 95 kDa Dichroic Ratios. *Top Right*: 95 kDa Aggregate Fractions. *Bottom Left*: 37 kDa Mobilities. *Bottom Middle*: 37 kDa Dichroic Ratios. *Bottom Right*: 37 kDa Aggregate Fractions.

Solutions of 37 kDa P3HT at concentrations of 2, 5, and 8 mg/ml were treated with UV irradiation and aging. After two days of aging, the average aggregate fraction of the 2 mg/ml solution was 16.2%, whereas those of the 5 and 8 mg/ml solutions were 11.9% and 9.51%, respectively. Thus, at lower concentrations, a larger fraction of polymer can crystallize, but less total crystalized polymer is in the solution. The dichroic ratios of the films made from these solutions showed a similar trend. The average dichroic ratio of the film made from the 2-day old 2, 5, and 8 mg/ml solutions were 2.22, 1.41, and 1.37 respectively. Thus, the polymer film treated in the 2 mg/ml solution was more optically active than those made from the other two solutions.

The long-range order of polymer films is a good indicator of the electrical capabilities of the corresponding film, but several other factors of the microstructure influence the electrical

capabilities. The charge-carrier mobilities of P3HT-coated transistors were measured to directly quantify their electrical performance. After 2 days aging, the 37 kDa P3HT films with the highest mobilities were those made from the 5 mg/ml solution, with an average mobility of 0.058 $cm^2/V*s$. Films produced from the 2-day-aged 2 and 8 mg/ml solutions showed very similar charge-carrier mobilities—0.039 and 0.038 $cm^2/V*s$, respectively. Thus, the 37 kDa P3HT processed in a 5 mg/ml solution showed neither the highest aggregate fraction nor the highest dichroic ratio, but outperformed the competition in charge-carrier mobility. Thus, neither the extent of aggregation nor the film's optical activity appear to be sole predictors of a film's electrical capabilities.

Table I: Details of Solution Aggregation

Solution Parameters			0 days		2 Days	
MW (kDa)	Concentration (mg/ml)	Molar Concentration (mM)	Aggregate Fraction (%)	Mass of Aggregated Polymer (mg/mL)	Aggregate Fraction (%)	Mass of Aggregated Polymer (mg/mL)
37	2	0.054	11.6	0.23	16.2	0.32
37	5	0.135	7.2	0.36	11.9	0.59
37	8	0.216	6.5	0.52	9.5	0.76
95	2	0.021	23.7	0.47	27.1	0.54
95	4	0.042	18.1	0.72	25.4	1.02
95	5	0.053	13.1	0.66	23.6	1.18

95 kDa P3HT was studied with the same methods, but at solution concentrations of 2, 4, and 5 mg/ml. Solutions showed higher dichroic ratios, higher aggregate fractions, and higher mobilities than those created with the lower weight. Longer aging resulted in higher aggregate fractions and higher dichroic ratios for all solutions of 95 kDa P3HT. After 2 days of aging, the 2, 4, and 5 mg/ml solutions of 95 kDa P3HT had aggregate fractions of 27.1%, 25.4%, and 23.6%, respectively. Likewise, the dichroic ratios of films of P3HT processed in 2, 4, and 5 mg/ml solutions were 3.05, 2.77, and 2.13, respectively. As was seen in the 37 kDa P3HT, higher-concentration solutions led to more polymer aggregation and better directional order in films.

However, as was seen in the 37 kDa P3HT, neither higher aggregation nor more directional order necessarily translated to higher mobilities. Immediately after UV treatment, the films had average mobilities of 0.042, 0.074, and 0.056 $cm^2/V*s$ for the 2 mg/ml, 4 mg/ml, and 5 mg/ml solutions, respectively. For these same solutions, but after 2 days of aging, the mobilities of films produced from the 2, 4, and 5 mg/ml solutions averaged 0.071, 0.069, and 0.072 $cm^2/V*s$, respectively. The average mobilities after two days aging were not statistically different, but those of the unaged mobilities were. Immediately after UV treatment, the mobilities of the solutions showed the same relationship as was seen in the preliminary experiments. The peak mobility was seen in the film made from the 4 mg/ml solution. Even though the aggregate fractions and dichroic ratios were greater for the 2 mg/ml solution, the mobilities were relatively low with no aging. It is noteworthy that the aging had an unexpected effect on the mobility of the 4 mg/ml solution; films produced from the unaged solution had a higher charge-carrier mobility. This is inconsistent with results seen in other experiments and was not seen in preliminary studies. This was likely a result of error.

iii. Results: AFM Image Analysis

AFM images were taken to further analyze the microstructures of the P3HT films. The raw AFM images are presented in Appendix B. Images of the 37 kDa P3HT films did not show any fibril structures on day 0, so they are not included. All images collected were analyzed to determine, among other parameters, the mean fiber length and width and the long-range directional alignment. The data is presented in Figure 7.

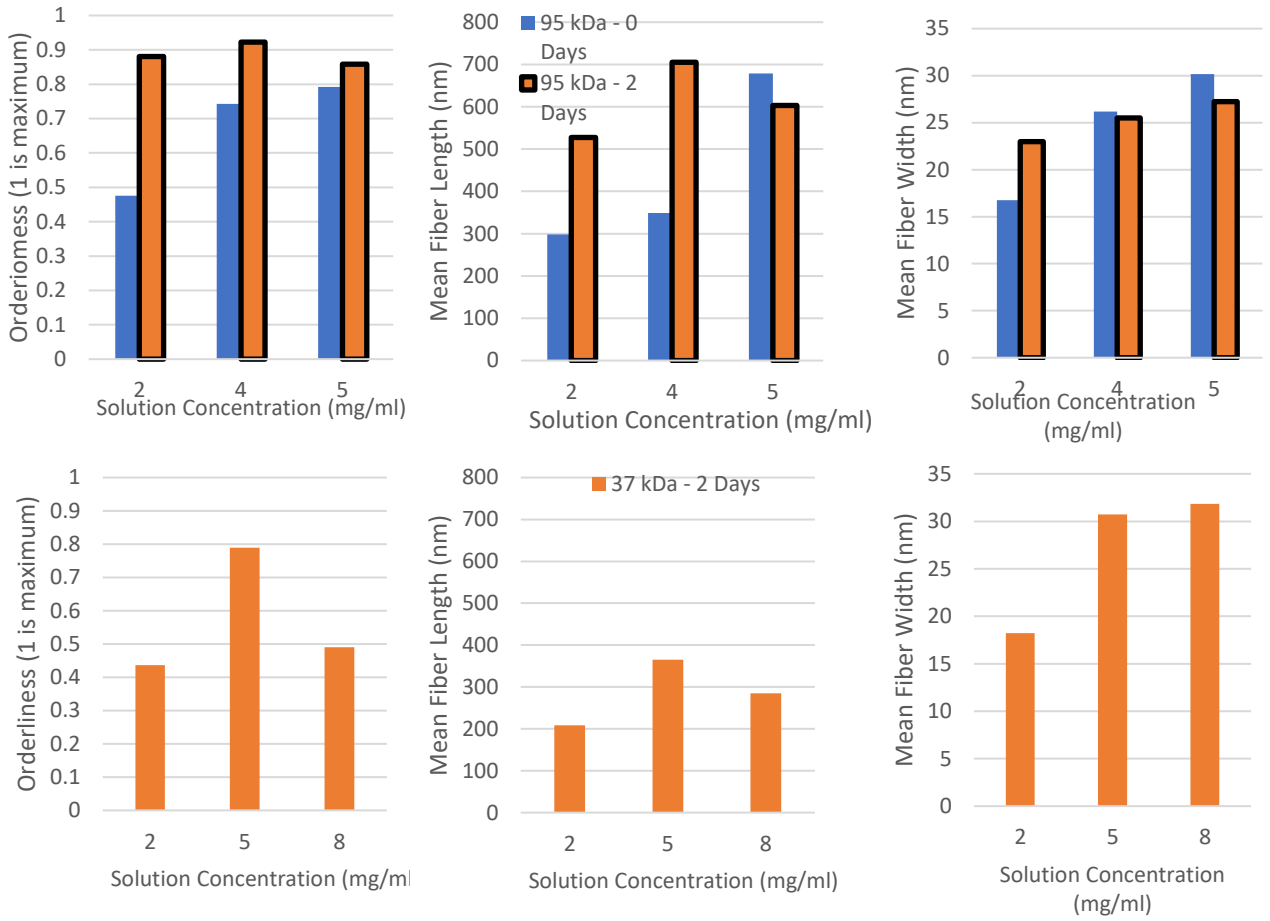

Figure 7. Mean fiber length, mean fiber width, and directional order as a function of solution concentration and aging.

Initially, higher concentration led to longer fibers. Immediately after UV-treatment, the 5 mg/ml 95 kDa solution had the longest and thickest fibers with an average length and width of 679x30 nm. The average lengths and widths of the 2 and 4 mg/ml solutions were 298x16 and 349x26 nm, respectively. However, over the next two days, neither the width nor length of the fibers in the 5 mg/ml solution changed appreciably. After aging, the average widths still depended on concentration, but the average lengths did not. The mean fiber widths after 2 days of aging was 23, 25, and 27 nm for the 2, 4, and 5 mg/ml solutions, respectively; the mean lengths were 527,

705, and 603 nm for the 2, 4, and 5 mg/ml solutions, respectively. Thus, the middle concentration had the longest chains after aging.

For the 37 kDa P3HT, AFM images could not effectively see the fibril structure of the unaged solutions; thus, images were only collected after 2 days aging for this molecular weight. The 37 kDa polymer showed trends like those of the 95 kDa P3HT. For both molecular weights, more concentrated solutions produced thicker chains. The average widths of polymers from the 2, 5, and 8 mg/ml solutions were 18, 31, and 32 nm, respectively. Furthermore, the longest fibers were in polymers from the middle concentration tested. The lengths of the 2, 5, and 8 mg/ml solutions were 208, 364, and 284 nm, respectively.

The molecular weight of the polymer did not seem to affect the width of the nanofibers; the average fiber width of the film produced from the 5 mg/ml solution of 95 kDa P3HT was approximately 27 nm, while that produced from the 5 mg/ml solution of 37 kDa P3HT was 30 nm. However, the average chain lengths did depend on the molecular weight of the polymer. The longest average fiber length seen in the 37 kDa P3HT films was only 365 nm, but the longest average chain length seen in films of the 95 kDa polymer was 705 nm. Thus, the molecular weight of the polymer appears to have a significant effect on the lengths of fibers, but not on the widths.

The high concentration solutions quickly formed thick, long fibers that did not change significantly over the next 2 days. The lower concentration the concentration, the faster the fiber length grew during aging. These relations between the fiber growth and solution concentrations agree with kinetic theory. At higher concentrations, more intramolecular collisions lead to faster growth of the fibers in all directions. Thus, films made from more concentrated solutions initially created wider and longer fibers. However, after the initial period of fast growth, the longitudinal

growth of fibers in the more concentrated solutions is inhibited by steric hindrance. By the end of the second day, differences in fiber size were less extreme, but present nonetheless.

In addition to the fibers' sizes, the coefficient of directional order was also extracted from the AFM images. For the films created from 37 kDa P3HT, the 5 mg/ml solution had both the best order and the longest fibers. This is in accordance with the mobility data, in which the 5 mg/ml solution performed best electrically. Neither the 2 mg/ml nor the 8 mg/ml solution of 37 kDa P3HT produced well-ordered fiber structures; this failure to create effective microstructures is reflected by the poor electrical measurements of these films. For the 95 kDa P3HT, the directional order for

The clearest effect of solution concentration on crystal microstructure was its relationship with the fiber thickness. At higher concentrations, the fibers were wider for all films observed. However, the fiber width has no significant impact on mobility. Chain lengths had some influence on mobility, but only seemed to make a significant difference if the fibers were very short, in which case the mobility was low.

In addition to the correlations identified so far, an interesting relationship was also seen between the AFM image data and the mobilities; this is presented in Figure 8. The fiber length of chains in day 2 films correlated with the mobilities of films created from the unaged solutions. For both the 35 kDa P3HT, 95 kDa P3HT, and the sample set of both, the mobility on day 0 was closely correlated with the fiber length on day 2, with a n R-squared value of 0.9. The exact reason for this correlation is unknown, but the trend is interesting nonetheless.

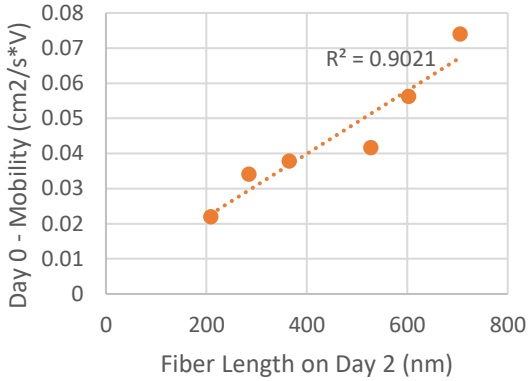

Figure 8. Correlation of mobility on day 0 and fiber length on day 0 for both 37 and 95 kDa P3HT.

iv. Discussion of Error

The methods used in this experiment had many issues with reproducibility. Although the UV-vis measurements were generally consistent, mobilities sometimes differed drastically. In several solutions, P3HT precipitated, interrupting the ordered crystal lattice. Those films that demonstrated precipitation almost always had very low mobilities around 0.02 $cm^2/V*s$. These samples were removed from the data sets as outliers for all averages taken, but their occurrence is noteworthy nonetheless. Precipitation was neither seen in the devices made from unaged solution nor in those made from 37 kDa P3HT. However, each concentration of 95 kDa P3HT solution produced at least one film that displayed precipitation.

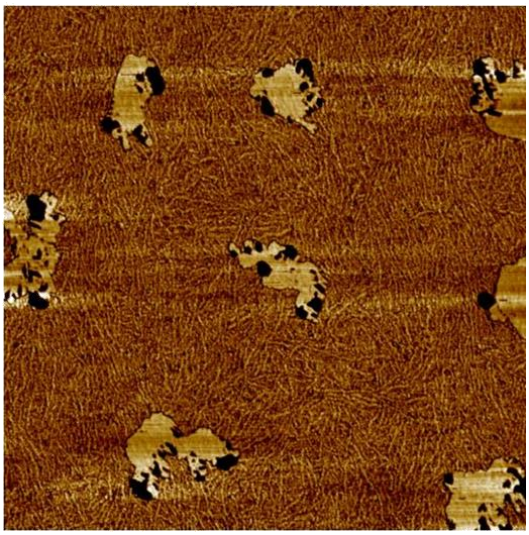

Figure 9. An AFM image of a film showing precipitation. The gold splotches on the film are P3HT precipitate.

The cause of the precipitation remains unclear. Most variables were closely monitored but a few proved difficult to control. My top theory for the cause of the precipitation is contamination prior to UV-treatment. Several items, including tweezers, stir bars, and storage boxes, were only cleaned with rinses of methanol and isopropyl alcohol between consecutive trials; this introduces the possibility of contamination, which would be a possible explanation for why some films displayed precipitates. If an initial bit of crystalized polymer makes its way into a solution prior to treatment, it will increase the initial rate of crystallization. This would explain why the precipitation was not seen immediately after UV-treatment, but was seen two days later. These specks could have catalyzed chain growth, resulting in precipitation during the aging.

There were several other small sources of random error. While blade coating, the width of the blade often differed between consecutive experiments. Although the height of the blade remained relatively constant, the behavior of the solution front was probably affected by the width applying the shear force. It could not reach all portions of the vial equally and often got stuck during treatment. These inconsistencies in the stirring of the solution may have led to some chains being exposed to more UV irradiation than others, leading to uneven aggregation.

VII. CONCLUSIONS

i. Analysis

The optimum processing of P3HT may have no one correct answer, but each new study pushes the field closer. Countless variables influence the polymer's properties, and the methods used to analyze P3HT are sensitive and time-consuming. This experiment initially sought to investigate the role of solution concentration on P3HT properties. Several experiments were completed, employing numerous methods to analyze the P3HT. However, it can be concluded that solution concentration has a direct relationship with the physical properties of P3HT fibers, but not necessarily on the electrical abilities. Thus, to claim an optimum concentration for P3HT solutions would be an oversimplification.

Concentration had strong influences on details of the polymer crystals. A lower percentage of polymer crystalized in solutions of high concentrations, but by mass, there was still more aggregated polymer in these concentrated solutions. Fiber lengths after aging were similar at all concentrations, but the initial growth of fibers under UV-irradiation was faster at higher concentrations. Fiber widths, however, grew steadily with concentration for both molecular weights of P3HT. Optical activity was highest for films with low concentrations, and yet the directional alignment seen in under AFM showed no direct relationship.

The fiber width, fiber length, aggregate fraction, and dichroic ratio showed obvious trends with concentration, but demonstrated little relation to mobilities. The only variable that correlated closely with electrical capabilities was directional alignment. Generally, the most directionally ordered films were also those that performed best electrically. The polymer fibers were able to effectively order regardless of the fiber length or width and regardless of the solution concentration. No other parameter of the film microstructures correlated with either order or electrical abilities.

For the high molecular weight P3HT, mobilities peaked at the middle concentration, 4 mg/ml, before aging but were relatively constant for all concentrations after aging. For the lower molecular weight P3HT, mobilities also peaked at the middle concentration, 5 mg/ml, for both the unaged and aged solutions. The high effectiveness of the middle concentrations suggests an interplay between film density and steric hindrance in solution. At low concentrations, polymer chains in solution have more room to aggregate into fibers, resulting in a higher aggregate fraction. The mobilities appeared independent of the fiber lengths, but the day 0 mobilities correlated with the average fiber length on day 2.

This experiment has raised questions about the validity of dichroic ratio as a measurement of directional order. Technically, dichroic ratio is simply a measurement of the optical activity of a P3HT film, but it has been considered an effective measurement of a film's directional alignment. However, in this study, the dichroic ratio did not correlate with the directional alignment parameter determined from the AFM images. The optical activity of the films was far more related to the concentration of the solutions and molecular weight of the polymer. However, the concentration did not seem to directly impact the order of fibers seen under AFM.

This study has also raised several further questions regarding the role of aggregation in a film's microstructure. Although some aggregation is necessary, too much aggregation seems undesirable. There appears to be an optimal point of aggregation, rather than an optimal concentration. The aggregation relies on the aging, concentration, molecular weight, solution volume, and numerous other parameters, so quantifying this ideal aggregation is difficult.

Reproducibility remains a significant problem due to the precision of the instrumentation involved, and precipitation presents further challenges for the industry. Faulty devices were more common at higher molecular weights and after aging. Higher molecular weight generally led to higher mobilities, however, the 95 kDa P3HT showed precipitation more often. Although the specific cause of the precipitation remains unknown, steps can be taken to avoid it. Most importantly, the P3HT solution should be mixed sufficiently during UV-treatment and all materials should be thoroughly cleaned.

ii. Future Experimentation

In hindsight, there are several changes that would have improved this study. The most promising improvement to the current experimental design would be to automate the systems involved, removing several sources of human error. Especially during blade coating, a small random error can be detrimental to the device's electrical properties. More precise instrumentation would decrease the variability encountered due to random error. Another potential improvement to the experiment would implement better cleaning methods for all supplies. Cleaning the stir bars with sonication and/or ozone would ensure that no impurities would be introduced into the P3HT solutions or films.

In addition to potential improvements to experimental methods, several correlations could be better understood with further studies. Though an optimum concentration may not exist, there

may be an optimum extent of aggregation. It would be interesting to further investigate the relationship between solution aggregation and fiber details, including length, width, and density. None of these parameters had direct correlations with mobility, but they may relate the fibers are dispersed during blade coating. Furthermore, an intriguing investigation would be on solution concentration, focusing more on the films' microstructures than electrical properties. It has been documented several times that fiber order is closely related to electrical capabilities of a polymer film, so the identification of processing details that specifically result in ordered films is desirable.

VIII. APPENDIX A: Data Analysis Methods

i. OFET Creation

Organic Field Effect Transistors (OFETs) with bottom-gate bottom-contact design were created from highly n-doped silicon wafers that served as the gate. The capacitor layer consisted of a 300-nm thick layer of silicone dioxide, and the electrodes were composed of 50-nm thick gold (Au) with a 3 nm thick chromium (Cr) adhesive layer. The gold and chromium were deposited on the OFET via photolithography followed by E-beam evaporation onto the silicone dioxide (SiO_2). Prior to deposition of the P3HT, the OFETs were cleaned in an ultrasound sonication bath, rinsed with methanol and isopropanol, and then exposed to UV-ozone (Novascan PSD-UV).

ii. Aggregate Fraction Calculation

A UV spectrum was obtained through previously described methods. The spectrum was normalized and the measurements were fitted to a Frank-Condon progression using Equation A2:

$$A(E) \propto \sum_{m=0} \left(\frac{S^m}{m!}\right)\left(1 - \frac{We^{-S}}{2E_p}\sum_{n\neq m}\frac{S^n}{n!\,n-m}\right)^2 \exp\left(\frac{\left(E - E_{0-0} - mE_p - \frac{1}{2}WS^m e^{-S}\right)^2}{2\sigma^2}\right) \quad \text{(A2)}$$

where W is the exciton bandwidth, $E_{0\text{-}0}$ is the 0-0 transition energy, σ is the Gaussian linewidth, m is the number of vibrational transitions, n is the number of chromophores, S is the Huang-Rhys factor (set to 1), and E_p is the effective energy of the vinyl stretch mode (fixed to 0.179 eV). This equation was fitted to the lower energy part of the spectrum by changing the variables W, $E_{0\text{-}0}$, σ, and k, and optimizing the fit with the MATLAB function *lsqcurvefit*.

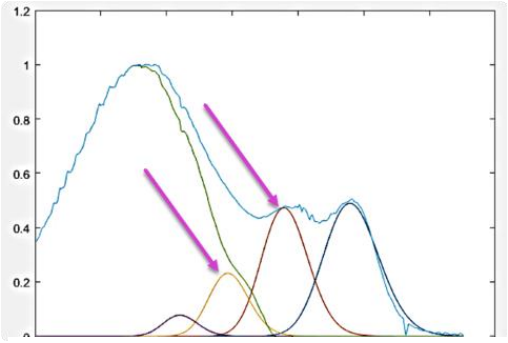

Figure A1. Aggregate fraction calculation using Frank-Condon progression.

iii. Mobility Calculation

The OFETs were measured and the charge-carrier mobilities were calculated in the saturation regime using Equation A3:

$$I_{DS} = \frac{WC_{ox}}{2L}\mu(V_{GS} - V_{th})^2 \quad \text{(A3)}$$

where I_{DS} refers to the drain current, V_G refers to the gate voltage, W and L are the channel width and length, respectively, μ refers to the hold mobility, V_{th} refers to the threshold voltage, C_{ox} refers to the capacitance per unit area of the silicone gate. The values of W, L, and C_{ox} were 50 μm, 2000 μm, and 1.15×10^{-8} F cm^{-2}, respectively.

iv. AFM Image Analysis

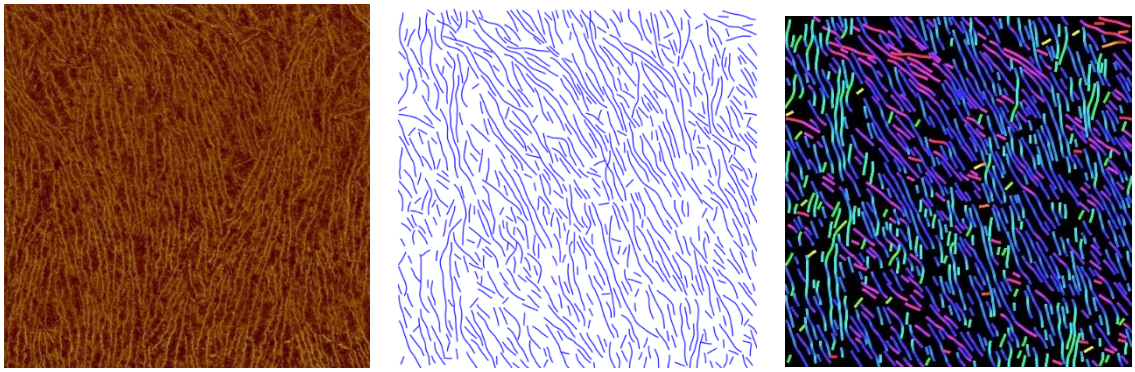

Figure A2. The process of cleaning an AFM image. (left) A raw AFM image. (middle) The skeletal structure of the fibers of the film. (right) The skeletal structure color-coded based on vector direction.

A MatLab function developed by Nils Pearson is used to analyze the fibril structures of the P3HT films. The function inputs a raw AFM image and outputs details including the directional alignment and mean fiber length. The code first cleans the image based on color gradients, producing an image such as the middle picture in Figure Z. The program analyzes this skeletal structure of the films by fitting a linear vector to each segment. By analyzing the angles of each fiber, the program determines the overall directional alignment of the film. The right image in Figure Z depicts a visual of the directional order.

IX. APPEXDIX B: Raw AFM Images

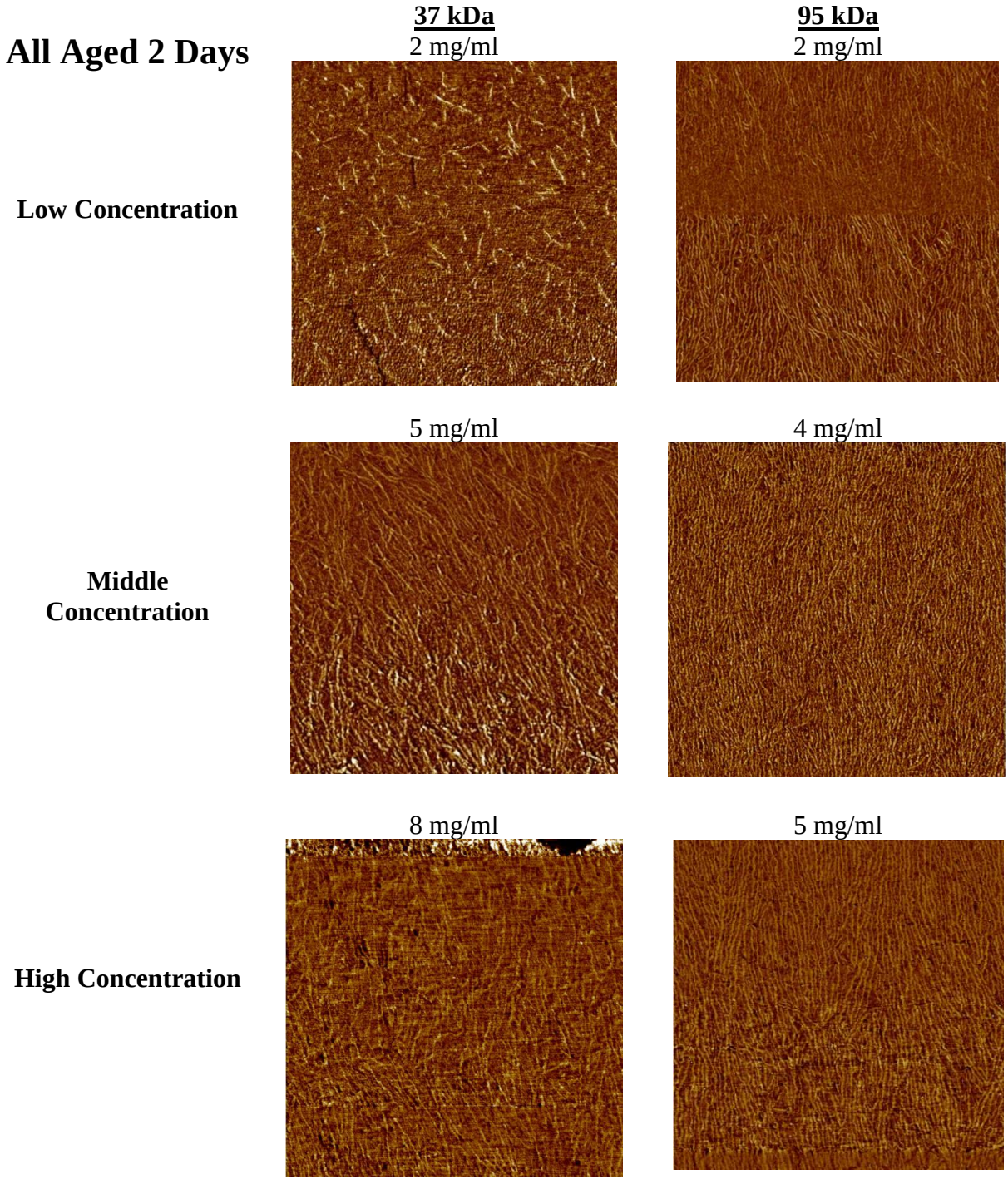

Figure B1. Raw AFM Images of films produced from the 2 day-aged P3HT.

Figure B2. Raw AFM Images of films produced from the unaged P3HT. No images were collected for the 37 kDa P3HT because of a lack of obvious structure.

X. REFERENCES

1. Ando, H. S. a. M., Materials challenges and applications of solution-processed organic field-effect transistors. *MRS Bulletin* **2008,** *33*, 676-682.
2. Nabil Kleinhenz, C. R., Sourav Chatterjee, Mincheol Chang, Karthik Nayani, Zongzhe Xue, Eugenia Kim, Jamilah Middlebrooks, Paul S. Russo, Jung Ok Park, Mohan Srinivasarao, Elsa Reichmanis, Liquid Crystalline Poly(3-hexylthiophene) Solutions Revisited: Role of Time-Dependent Self-Assembly. *Chemistry of Materials* **2015,** *27* (7), 2687-2694.
3. Malenfant, C. D. D. a. P. R. L., Organic thin film transistors for large area electronics. *Advanced Materials* **2002,** *14* (2), 99-117.
4. Sirringhaus, H., Device physics of solution-processed organic field-effect transistors. *Advanced Materials* **2005,** *17*, 2411-2425.
5. Rees, H. D., Field effect transistors. Google Patents: 1980.
6. H. Koezuka, A. T., T. Ando, Field-effect transistor with polythiophene thin film. *Synthetic Materials* **1987,** *18*, 699-704.
7. Jung Ah Lim, J.-H. K., Longzhen Qiu, Wi Hyoung Lee, Hwa Sung Lee, Donghoon Kwak, Kilwon Cho, Inkjet-printed single-droplet organic transistors based on semiconductor nanowires embedded in insulating polymers. *Advanced Functional Materials* **2010,** *20*, 1-6.
8. Ping-Hsun Chu, N. K., Nils Persson, Michael McBride, Jeff L. Hernandez, Boyi Fu, Guoyan Zhang, Elsa Reichmanis, Toward Precision Control of Nanofiber Orientation in Conjugated Polymer Thin Films: Impact on Charge Transport. *Chemistry of Materials* **2016,** *28*, 9099-9109.
9. Rodrigo Noriega, J. R., Koen Vandewal ,Felix P.V. Koch, Natalie Stingelin, Paul Smith, Michael F. Toney, Alberto Salleo, A general relationship between disorder, aggregation and charge transport in conjugated polymers. *Nature Materials* **2013,** *12*, 1038-1044.
10. Jiangang Liu, Y. S., Xiang Gao, Rubo Xing, Lidong Zheng, Shupend Wu, Yanhou Geng, Yachun Han, Oriented Poly(3-hexylthiophene) nanofibril with the pi-pi stacking growth direction by solvent directional evaporation. *Langmuir* **2011,** *27*, 4212-4219.
11. John E. Anthony, A. F., Martin Heeney, Seth R. Marder, Xiaowei Zhan, n-Type organic semiconductors in organic electronics. *Advanced Materials* **2010,** *22*, 3876-3892.
12. Mincheol Chang, J. L., Nabil Kleinhenz, Boyi Fu, Elsa Reichmanis Photoinduced anisotropic supramolecular assembly and enhanced charge transport of poly(3-hexylthiophene) thin films. *Advanced Functional Materials* **2014,** *24*, 4457-4465.
13. Mincheol Chang, D. C., Eilaf Egap, Macroscopic Alignment of One-Dimensional Conjugated Polymer Nanocrystallites for High-Mobility Organic Field-Effect Transistors. *Applied Materials & Interfaces* **2016,** *8*, 13484-13491.
14. Nils Persson, M. M., Martha Grover, Elsa Reichmanis, Silicon Valley meets the ivory tower: Searchable data repositories for experimental nanomaterials research. *Solid State and Material Science* **2016**.
15. Christina Scharsich, R. H. L., Michael Sommer, Udom Asawapirom, Ullrich Scherf, Mukundan Thelakkat, Dieter Neher, Anna Kohler Control of aggregate formation in poly(3-hexylthiophene) by solvent, molecular weight, and synthetic method. *Journal of Polymer Science* **2011,** *50* (6), 442-453.
16. Persson, N. E.; McBride, M. A.; Grover, M. A.; Reichmanis, E., Automated Analysis of Orientational Order in Images of Fibrillar Materials. *Chemistry of Materials* **2017,** *29* (1), 3-14.